Ninth Canadian Conference on Earthquake Engineering
Ottawa, Ontario, Canada
26-29 June 2007

EFFECT OF THE VERTICAL EARTHQUAKE COMPONENT ON THE SEISMIC RESPONSE OF REINFORCED CONCRETE MOMENT FRAMES

M.A. Elfeki[1] and M.A. Youssef[2]

ABSTRACT

The seismic behaviour of multi-storey Reinforced Concrete (RC) structures under the effect of horizontal excitations has been the subject of extensive studies over the last several decades. Due to the increase in near-source records, researchers recently emphasized the importance of the vertical earthquake component. In this paper, a comparative study of the inelastic seismic performance of a six-storey RC building under the effect of the horizontal earthquake component and both the horizontal and vertical components is carried out. Six earthquake records are used to study the global and local inelastic behaviour of the building. It is concluded that considering the vertical component does not have significant effect on the computed drift, but greatly affects the distribution and intensity of local damage. It is essential to include the vertical component of earthquakes to accurately predict the ductility of the structure and its expected failure mechanism.

Introduction

The vertical component of earthquake records was usually neglected while designing RC buildings. Recently, after the increase of near-fault records, a number of building codes (Eurocode 8 1998 and IBC 2000) provided an estimate for the vertical design response spectra as 2/3 of the horizontal design spectra. Many researchers (Abrahamson and Litehiser 1989, Papazoglou and Elnashai 1996) concluded that this estimate could result in un-conservative values as the ratio between the vertical and horizontal ground accelerations (V/H) for many records such as 1989 Loma Prieta and 1994 Northridge were higher than 1.0. The V/H ratio depends on the earthquake magnitude and on the epicenteral distance (Papazoglou and Elnashai 1996). This underestimation of the vertical component of ground motion may lead to unexpected seismic damage in buildings located near the faults.

The main objective of this study is to investigate the effect of the vertical earthquake component on the response of a RC building located in a high seismicity region. A six-storey building located in California was designed according to ACI requirements (ACI 318 2002). The designed building was subjected to a static pushover analysis to define the limits of the global damage states. Incremental dynamic analyses using six ground motion records were conducted to compare the seismic response of the building for horizontal excitations and for horizontal and vertical excitations.

[1] Ph.D. Candidate, Dept. of Civil & Environmental Eng., The Uni. of Western Ontario, London ON., N6A 5B9
[2] Assistant Professor, Dept. of Civil & Environmental Eng., The Uni. of Western Ontario, London ON., N6A 5B9

Six-storey RC building

A symmetric six-storey RC office building is used for the analysis. The selected dimensions and layout of the building are shown in Fig. 1.

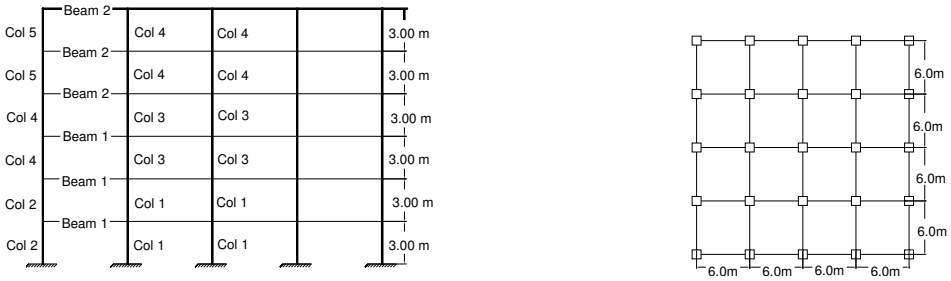

Figure 1. Six-Storey building.

The building was located in California. It was designed according to the regulations of the International Building Code (IBC 2000) and the ACI requirements (ACI 318 2002) for both gravity and seismic loads. The concrete compressive strength was assumed 28 MPa and the yield strength of the reinforcing bars was considered 400 MPa. The dead load included the weight of the structural elements and the masonry walls. The live load was 3.83 KN/m^2. The moment frame was designed for the critical load combination as a special moment frame. Chosen sizes for beams and columns and reinforcement details are given in Fig. 2.

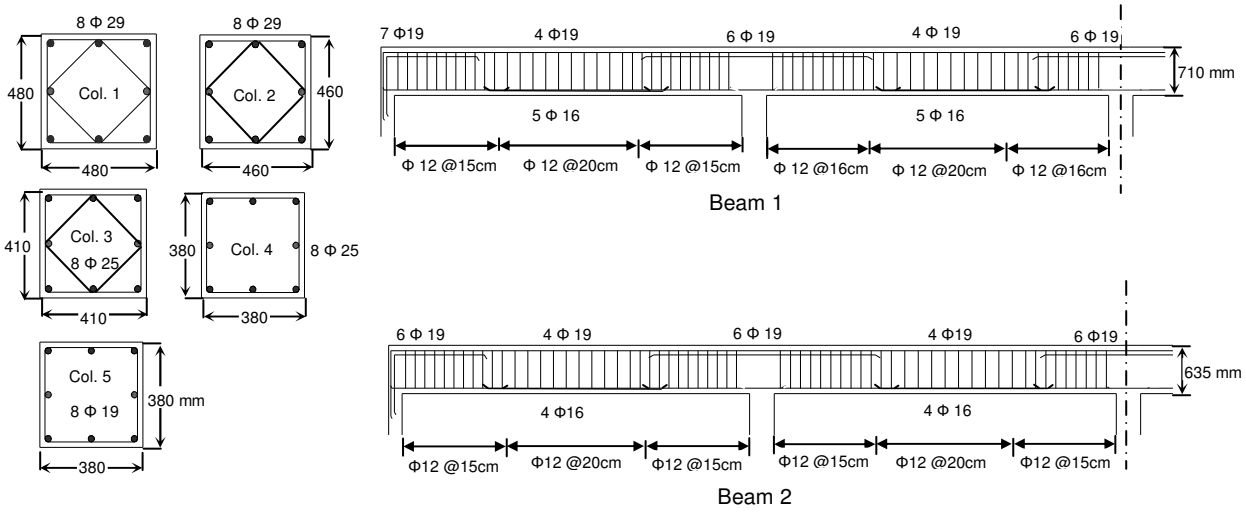

Figure 2. Reinforcing details.

Analytical Modeling

The finite element program ZEUS-NL (Elnashai et al 2002) was utilized to perform the pushover and the nonlinear dynamic analyses. The program is capable of representing spread of inelasticity within the member length using the fiber analysis approach and can be used to predict the nonlinear response of moment frames under static or dynamic loading. Accurate concrete and steel material models are available in the program library. The program has been tested and validated by others (Jeong and Elnashai 2005).

Because of the symmetry of the building, a 2D model was used to idealize a typical moment frame. Some assumptions and techniques were adopted. Beams and columns were modeled using cubic elasto-plastic elements. Each beam element was divided into five elements to model the variation in the longitudinal and transverse reinforcements. Each column element was divided into three elements, two end elements and

one intermediate element. The effective flange width of the beams was assumed to be equal to the beam width plus 14% of the clear span (Jeong et al. 2005). Rigid elements were used to model beam-column connections as shown in Fig. 3a. For edge beam-column connections, where the size of the column was changing, a different arrangement of rigid arms was used as illustrated in Fig. 3b.

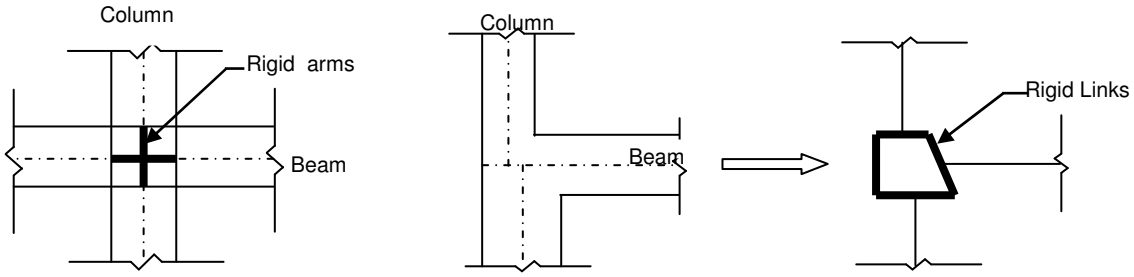

a) Intermediate beam column connection b) Edge beam column connection

Figure 3. Rigid arms for modeling of beam-column connections.

Yielding and Crushing Limit States

Local yielding of elements is defined when the tensile strain in the longitudinal reinforcement reaches its yield strain (ε_y= 0.002). Many criteria were suggested by different researchers to identify concrete crushing of individual members. This includes using a value for ultimate curvature or assuming that the crushing strain is 0.003 (Mwafy and Elnashai 2001). The crushing strain is expected to depend on the type of concrete and the confinement. The crushing strain was found to be varying from 0.0025 to 0.006 for unconfined concrete (Macgregor and Wight 2005) and from 0.015 to 0.05 for confined concrete (Paulay and Priestley 1992).

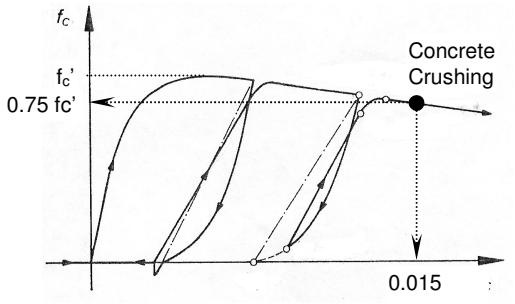

Figure 4. Confined concrete stress-strain curve (Mander et al. 1988).

The concrete stress-strain curve for confined concrete including unloading and reloading branches is shown in Fig. 4. The envelope to this curve is very close to the stress-strain curve for monotonic test (Macgregor and Wight 2005). For the designed cross-sections (Fig. 2), crushing was assumed to occur when the confined concrete strain reaches 0.015. This value corresponds to a concrete stress of about 75% the peak stress as shown in Fig. 4.

Pushover Analysis

Inelastic pushover analysis was performed using ZEUS-NL. It allowed investigating the failure mechanism and determining the limit states of the moment frame. The vertical distribution of the lateral load was taken similar to the distribution used for the design. A force controlled pushover analysis was employed up to the maximum force resistance. For the post peak, the analysis proceeded by using displacement control.

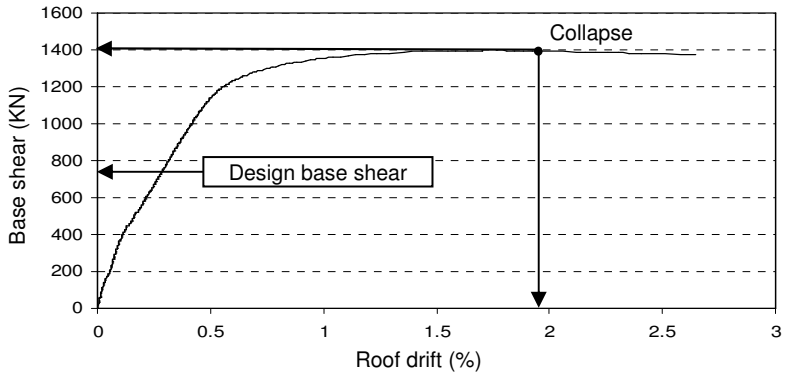

Figure 5. Relationship between roof drift and base shear.

Fig. 5 shows the pushover curve for a moment frame of the six-storey building. The building lateral capacity is 1.8 times the design base shear. Fig. 6 shows the distribution of interstorey drift over the building height at collapse. The maximum interstorey drift is observed in the second storey and is used to define the global damage levels. The relationship between the interstorey drift of the second floor and the base shear is shown in Fig. 7. The local damage of individual members was tracked and used to obtain the global limit states of the building. These limit states are illustrated in Fig. 7. The building remains elastic (no cracking) up to interstorey drift equal to 0.2%. Minor damage is expected for drifts between 0.2% and 1%. The 1% limit is taken as the point defining approximately the global yielding. At this drift, yielding was observed in the first three floors at the ends of all beams and few columns as shown in Fig. 8a. The extensive damage stage was observed to start at an interstorey drift of 2% as one of the columns was considered crushed. For storey drifts between 1% and 2%, the building is considered to be in moderate damage state. Fig. 7 shows that the second floor reaches its maximum capacity at 3% inter-storey drift, which is considered as the collapse limit if instability didn't occur before reaching this drift. This value is matching the value recommended by Broderick and Elnashai (1994) and Kappos (1997). At this level of drift, three columns were considered crushed (Fig. 8c). The damage limit states obtained from the pushover analysis in terms of interstorey drifts are matching the limits proposed by Hassanein (1997).

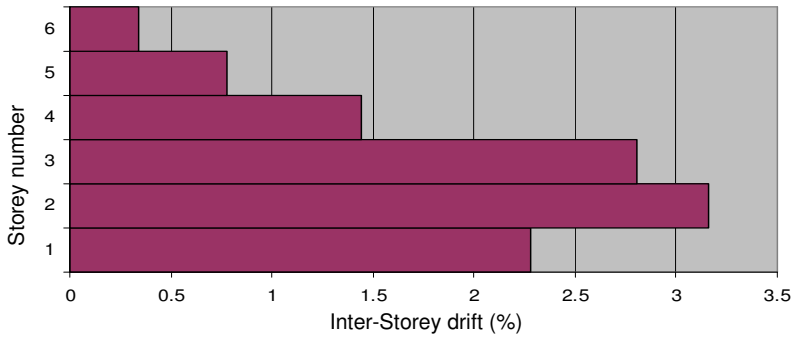

Figure 6. Interstorey drift distribution at collapse.

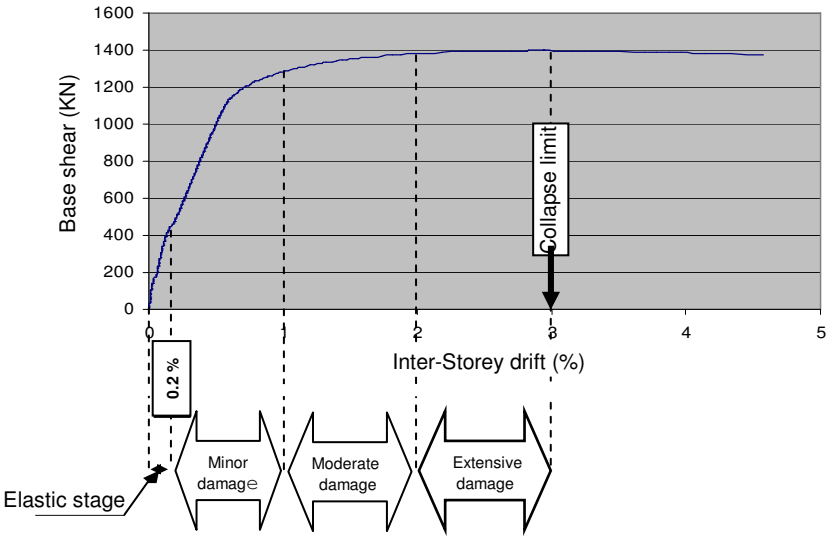

Figure 7. Relationship between interstorey drift and base shear.

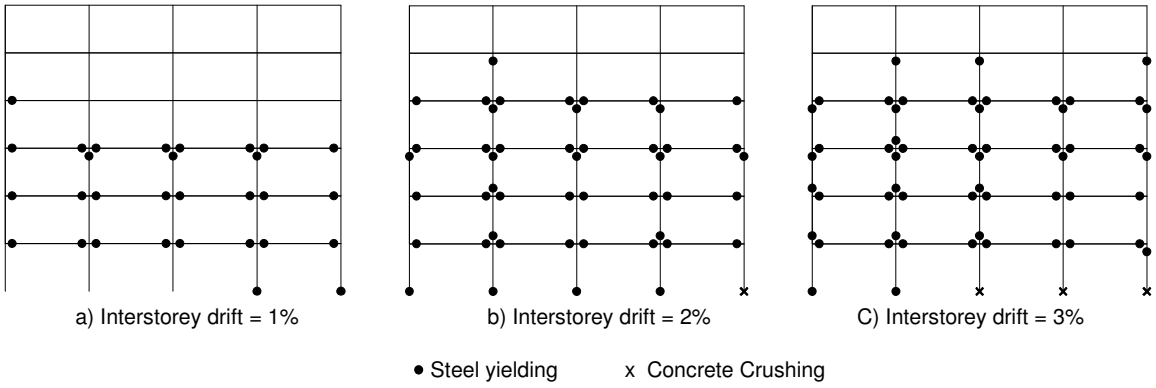

Figure 8. Local damage at different inter-storey drifts.

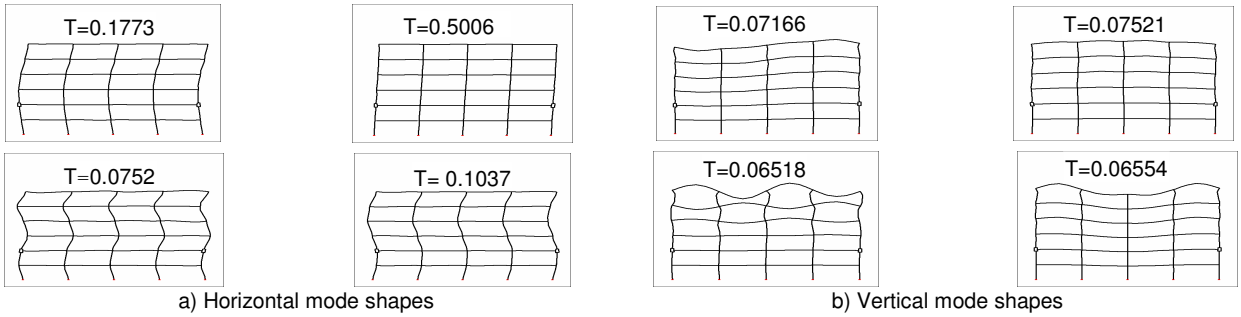

Figure 9. First four mode shapes of the six-storey RC building.

Seismic response analysis

Eigen value analysis was performed to determine the horizontal and the vertical periods of the structure. The fundamental horizontal and vertical periods of vibration were found equal to 0.5006 second and 0.0752 second, respectively. The first four mode shapes for both horizontal and vertical directions are shown in Fig. 9.

Selection of Ground Motion Records

Many researchers concluded that the vertical component of the earthquake has very significant effect on the seismic response of RC buildings located near the faults. This effect is influenced by V/H ratio, which might be greater than 1.0 (Bozorgnia and Niazi 1991, Niazi and Bozorgnia 1992; Abrahamson and Litehiser 1989). This ratio depends on the magnitude of the earthquake and the distance between the building under consideration and the earthquake centre (Collier and Elnashai 2001).

Six earthquakes records were selected to conduct dynamic analysis on the designed RC building. The records cover a wide range of ground motion frequencies as represented by the ratio between the peak ground acceleration and the peak ground velocity (A/v) and have V/H ratio greater than 0.6. The characteristics of the chosen records are presented in table 1. Every earthquake has three components, two in the horizontal direction (HL and HT) and one in the vertical direction (VL). To choose the effective horizontal component (HZ), the spectral accelerations for the two components were drawn and were compared at the fundamental period of the moment frame. The one with the higher value is selected for the analysis. Fig. 10 shows the spectral acceleration for the chosen earthquakes and the design spectra. Each of these records was considered twice (HZ only and HZ+VL).

Table 1. Chosen earthquake records.

Earthquake	Date	Magnitude (Ms)	Station	PGA (g)			V/H		A/v	
				HL	HT	HV	HV/HL	HV/HT	Class HL	Class HT
Northridge (USA)	17/1/94	6.7	Arleta-Nordhoff	0.31	0.34	0.55	1.79	1.6	High	Inter.
Imperial Valley (USA)	15/10/79	6.9	El Centro Array #6 (E06)	0.439	0.41	1.65	3.77	4.04	Low	Low
Loma Prieta (USA)	18/10/89	7.1	Capitola (CAP)	0.443	0.53	0.54	1.22	1.02	High	High
Whittier (USA)	1/10/87	5.7	Whittier Dam	0.316	0.23	0.51	1.6	2.21	High	High
Morgan Hill (USA)	24/4/84	6.1	Gillory Array #2 (G02)	0.212	0.16	0.58	2.73	3.6	High	High
San Fernando	9/2/71	6.6	Pacoima Dam	1.16	1.23	0.7	0.6	0.6	High	Inter.

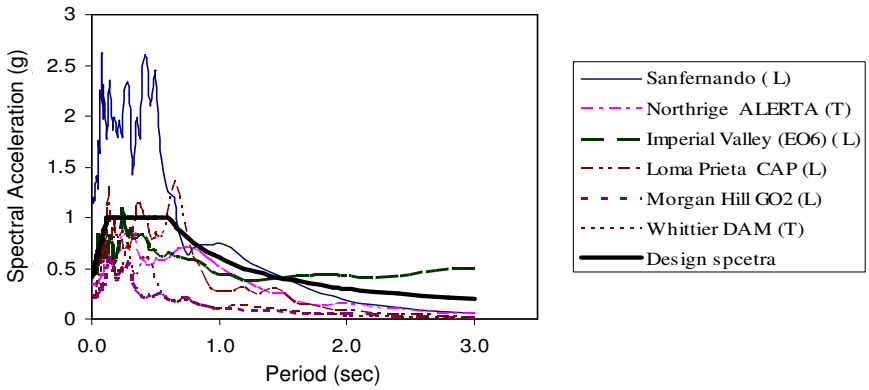

Figure 10. Spectral acceleration for the horizontal earthquake components and the design spectra.

Using a reliable method to scale the selected ground motion records is essential to conduct incremental dynamic analysis. Many methods have been proposed for scaling the ground motion records such as using the peak ground acceleration (PGA), Peak ground velocity (PGV), and the 5% damped spectral acceleration at the structure's first-mode period [Sa(T1, 5%)]. The structure is considered very stiff in the vertical direction and its seismic response is expected to be related to the ground acceleration. For such a case, using Sa(T1,5%) to scale the records is the most reliable method (Shome and Cornell 1999;

Vamvatsikos and Cornell 2002). Each component of the chosen earthquakes was scaled to different Sa(0.50056 second, 5%) levels and then used in the dynamic analysis.

Global Seismic Performance

Figs. 11 and 12 show the variation of the mean of the roof drift and the mean of the maximum interstorey drift with Sa(T, 5%). The figures show that the structure has almost the same roof and interstorey drifts at the same levels of Sa for the two cases of analysis. They also show that the moment frame reaches 3% interstorey drift at Sa(T, 5%) equals 1.35g.

Fig. 13 shows the relationship between the base shear and the mean roof drift for the six-storey building. The vertical excitation does not have noticeable effect on the roof drifts of the moment frame. The over-strength factor was calculated and found equal to 1.904 and 1.808 under the effect of horizontal excitations and horizontal and vertical excitations, respectively.

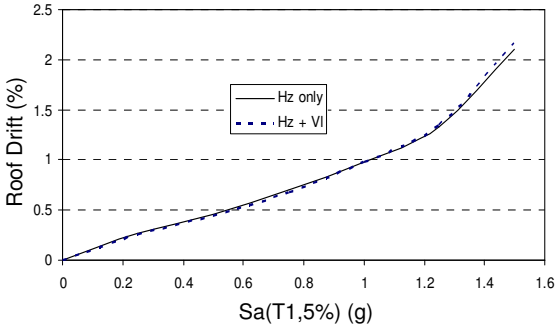

Figure 11. Variation of the roof drift with the spectral acceleration.

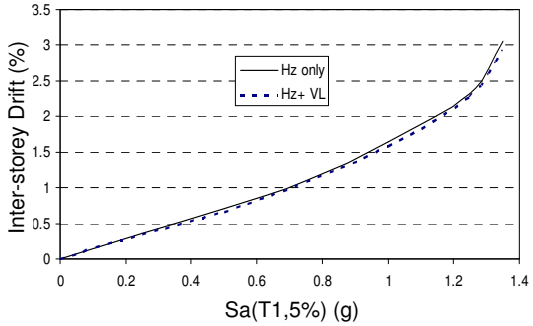

Figure 12. Variation of the Inter-storey drift with the spectral acceleration.

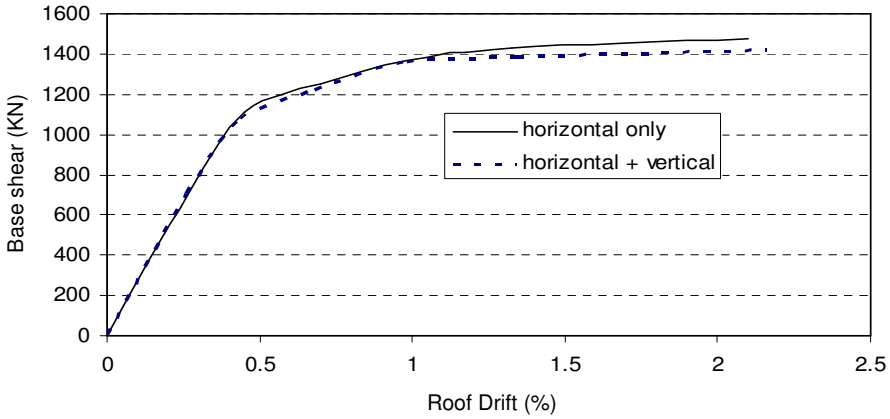

Figure13. Relationship between the base shear and the roof drift

Local Seismic Performance of the Building

Local damage of every individual element was tracked for yielding and crushing during the two cases of dynamic analyses. Fig. 14 shows the comparison between the damage occurred in the building beams and columns for the six earthquake records used in the analysis at 3% inter-storey drift. Table 2 shows the critical stories at which the maximum interstorey drift occurred. The location of the critical storey was affected by the frequency content of the considered earthquake.

It can be noticed from Fig. 14 that the level of damage is much higher when the vertical earthquake records are considered and that the interstorey drifts defining the response of the building need to be redefined. Analysis using the horizontal component only shows that no crushing has occurred in any of the beams. This is different from the case when both the horizontal and vertical components were considered for analysis. The local damage obtained from the figure shows that the moment frame is considered failed at an interstorey drift of 3% for all the chosen records except for Loma Prieta earthquake. This can be explained by the fact that the maximum interstorey drift for this case occurred at the fifth floor and thus the building can sustain higher levels of Sa.

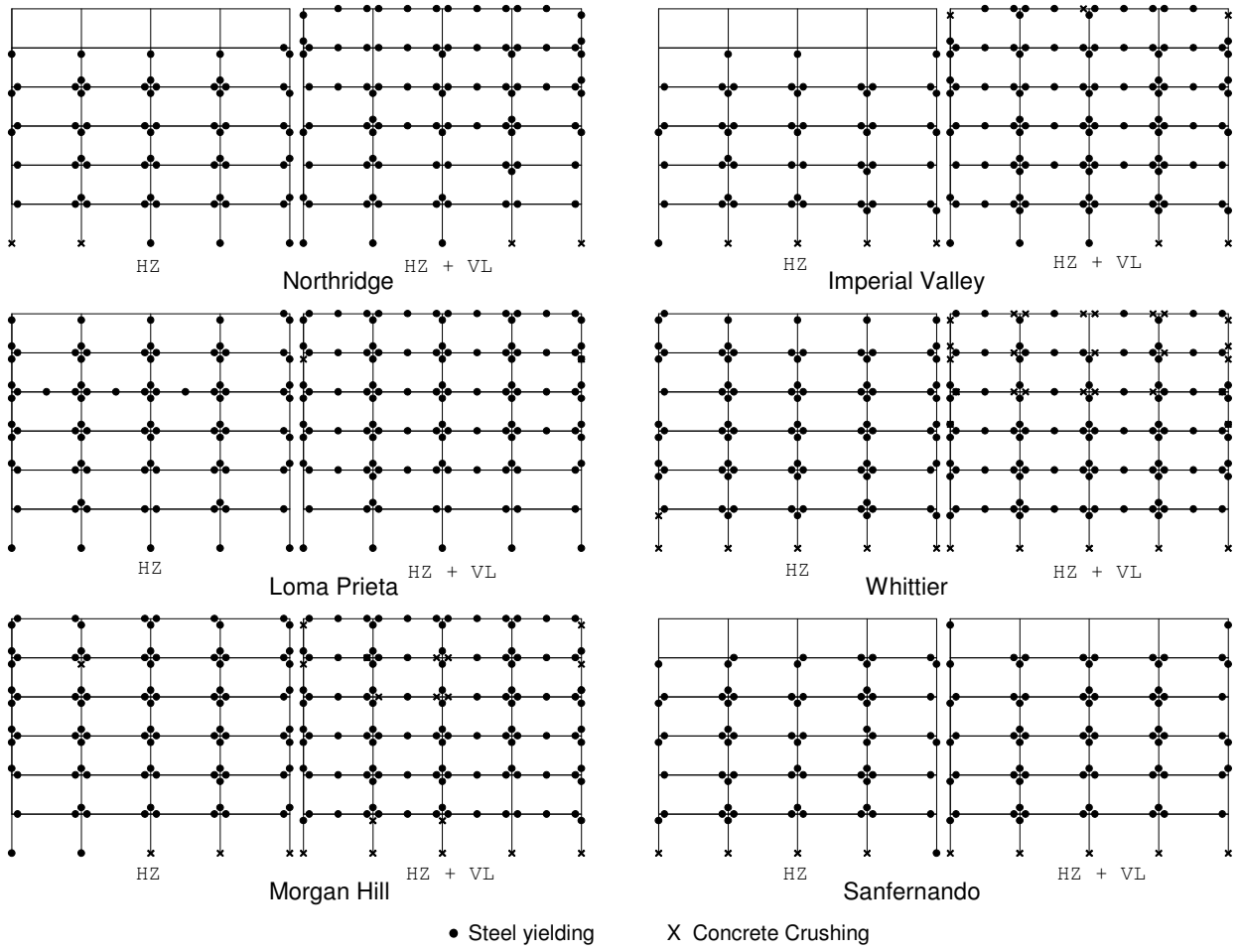

Figure 14. Damage in the RC building at 3% interstorey drift ratio.

Table 2. Number of the critical storey that sustained the maximum drift considering all records.

	Northridge		Imperial valley		Loma Prieta		Whittier		Morgan Hill		Sanfernando	
	HZ	HZ+VL	HZ	HZ+VL	HZ	HZ+VL	HZ	HZ+VL	HZ	HZ+VL	HZ	HZ+VL
Storey	3rd	2nd	2nd	2nd	5th	5th	1st	1st	3rd	3rd	2nd	2nd

Conclusions

In this work a six storey RC building was analyzed using pushover analysis to obtain the drift limits defining the response of the building. The building was then subjected to six different earthquake records. Nonlinear dynamic analyses were conducted using the effective horizontal component of each record and using both the horizontal and the vertical components. The local and global damages for the building were observed.

The results of the pushover analysis show that maximum inter-storey drift was obtained at the second storey. The building is elastic up to interstorey drift equal to 0.2% and reaches its maximum lateral capacity at interstorey drift of 3%.

It was observed from the dynamic analyses that the mean values of roof and interstorey drifts in the two cases of analysis are almost identical. It also shows that the maximum interstorey drift occurred at Sa(T,5%) equals about 1.35 times the design spectral acceleration. Under the effect of the horizontal excitation the over-strength factor of the building was 1.904, while it was about 1.808 under the effect of both the horizontal and the vertical components.

Including the vertical component in analyzing the building has resulted in extensive local damage (yielding of the reinforcing bars and crushing of the concrete). The drift limits defining the response of the building under the effect of horizontal earthquakes are not reliable for when the vertical component is included in the analysis.

Acknowledgements

This research was funded by the National Sciences and Engineering Research Council of Canada (NSERC). ZEUS-NL was developed at the Mid-America Earthquake Center using the National Science Foundation Award Number EEC-9701785.

References

Abrahamson, N. A. and J. J. Litehiser, 1989. Attenuation of vertical peak acceleration, *Bull. Seis. Soc. Am*. 79, 549-580.

ACI Committee 318, 2002. *Building code requirements for structural concrete,* (ACI 318-02) and commentary (ACI 318R-02), American Concrete Institute, Formington Hills MI, 444 pp.

Bozorgnia, Y. and M. Niazi, 1991. Behavior of near-source peak horizontal and vertical ground motions over SMART-1 array, Taiwan, *Bull. Seisn. Soc. Am*. 81(3).

Broderick, B. M. and A. S. Elnashai, 1994. Seismic resistance of composite beam-columns in multi-storey structures, Part 2: Analytical model and discussion of results, *Construction Steel Research* 30(3), 231–258.

Collier C. J. and A. S. Elnashai, 2001. A procedure for combining vertical and horizontal seismic action effects *Earthq Engrg* 5 ,(4), 521-539.

Elnashai, A. S., V. Papanikolaou, and D. H. Lee, 2002. ZEUS-NL User Manual, *Mid-America Earthquake Center (MAE) Report*.

Eurocode 8, 1998. *Design provisions for earthquake resistance of structures*. Part 1-1, 1-2 and 1-3, Comite Europeen de Normalisation, European Pre-standard ENV 1-1, 1-2 and 1-3, Bruxelles.

Hassanein A., 1997. Reliability Assessment of Rehabilitated Buildings of Moderate Height *M.Sc. Thesis,* McMaster University, Hamilton, Ontario, Canada.

IBC 2000, International Building Code, International code council, Falls Church, VA.

Jeong S.H., and A. Elnashai, 2005. Analytical Assussment of An Irregular RC Frame For Full-scale 3D Pseudo-Dynamic Testing Part I: Analytical Model Verification, *Earthq Engrg*. 9(1), 95-128.

Kappos, A. J. 1997. A comparative assessment of R/C structures designed to the 1995 Eurocode 8 and the 1985 CEB seismic code, *The Structural Design of Tall Buildings* 6(1), 59–83.

MacGregor, J. G. and J. K. Wight, 2005. *Reinforced Concrete Mechanics and Design* fourth edition.

Mander, J. B., M. J. Priestley, and R. Park, 1988. Theoretical stress-strain model for confined concrete ASCE, *Struct Engrg*. 114(8), 1804–1826.

Mwafy, A. M. and A. S. Elnashai, 2001. Static pushover versus dynamic collapse analysis of RC buildings, *Engrg. Struct.* 23(5), 407-424.

Niazi, M. and Y. Bozorgnia, 1992. Behavior of near-source vertical and horizontal response spectra at SMART-1 array, Taiwan, *Earthq. Engrg. Struct. Dyn*. 21, 37-50.

Papazoglou, A. J. and A. S. Elnashai, 1996. Analytical and field evidence of the damaging effect of vertical earthquake ground motion, *Earthq. Engrg. Struct. Dyn.* 25, 1109-1137.

Paulay, T. and M.J.N. Priestley, 1992., *Seismic Design of Reinforced Concrete and Masonry Buildings*, John Wiley & Sons, New York.

Shome N, C. A. Cornell, 1999. Probabilistic seismic demand analysis of non-linear structures, *Report No. RMS-35*, RMS program, Stanford University, Stanford, URL www.stanford.edu/group/rms/Thesis/

Vamvatsikos D. and C. A. Cornell, 2002. Incremental Dynamic Analysis, *Earthq Engrg and Struct Dyn.* 31, 491-514.